chemosensors

Article

Chemiluminescence Immunoassay for Sensitive Detection of C-reactive Protein Using Graphene Oxide–Gold Nanoparticle–Luminol Hybrids as Enhanced Luminogenic Molecules

Kyung Mi Kim [1,†], Phuong Thy Nguyen [1,†], Jeemin Kim [1], Seung Hoo Song [1], Jin Woo Park [2,*] and Moon Il Kim [1,*]

[1] Department of BioNano Technology, Gachon University, 1342 Seongnamdae-ro, Sujeong-gu, Seongnam 13120, Gyeonggi-do, Republic of Korea; kim_km17@naver.com (K.M.K.); nnphuongthy18@gmail.com (P.T.N.); jeem424@naver.com (J.K.); silencityland@gachon.ac.kr (S.H.S.)
[2] BioActs BM&S Co., Ltd., 80-59, Golden Root-Ro, Juchon-Myeon, Gimhae 50969, Gyeongsangnam-do, Republic of Korea
* Correspondence: park@bioactsbms.com (J.W.P.); moonil@gachon.ac.kr (M.I.K.)
† These authors contributed equally to this work.

Abstract: This study presents the development of luminol and gold nanoparticle co-functionalized graphene oxide (GO-AuNPs-L) hybrids as enhanced luminogenic signaling molecules in the chemiluminescence immunoassay (CLIA) for detecting C-reactive protein (CRP), a key biomarker of inflammation and cardiovascular diseases. When compared to free luminol, the GO-AuNPs-L hybrids significantly increased and prolonged the CL signal based on their synergistic enhancement in electron transfer during CL production. Based on the performance, the hybrids were employed as signaling molecules in both well plate-based and lateral flow CLIA platforms, showing substantial improvements in signal intensity and sensitivity in CRP detection. These results highlight the potential of GO-AuNPs-L hybrids as versatile and highly sensitive luminogenic molecules for immunological CRP detection, offering promising applications in clinical laboratory settings as well as in point-of-care diagnostics.

Keywords: chemiluminescence immunoassay; lateral flow immunoassay; CRP detection; luminol; graphene oxide; gold nanoparticles

Citation: Kim, K.M.; Nguyen, P.T.; Kim, J.; Song, S.H.; Park, J.W.; Kim, M.I. Chemiluminescence Immunoassay for Sensitive Detection of C-reactive Protein Using Graphene Oxide–Gold Nanoparticle–Luminol Hybrids as Enhanced Luminogenic Molecules. *Chemosensors* **2024**, *12*, 193. https://doi.org/10.3390/chemosensors12090193

Received: 18 August 2024
Revised: 9 September 2024
Accepted: 18 September 2024
Published: 20 September 2024

1. Introduction

Pentameric acute-phase C-reactive protein (CRP) is a key biomarker in the diagnosis and treatment of numerous inflammatory diseases, such as infections, chronic inflammatory disorders, and cardiovascular diseases [1]. As an indicator of systemic inflammation, elevated CRP levels in the bloodstream are strongly associated with an increased risk of adverse cardiovascular events, making their precise detection a crucial aspect of both preventive medicine and acute care [2,3]. Consequently, the development of advanced analytical methods for CRP detection has been a focal point in clinical diagnostics, with the goal of improving both the accuracy and efficiency of CRP measurement in diverse healthcare settings [4,5].

Currently, enzyme-based immunoassays are among the most widely utilized analytical techniques for CRP detection, owing to their high specificity and adaptability [5,6]. These assays frequently employ peroxidases, such as horseradish peroxidase (HRP), as labeling enzymes due to their robust catalytic activity and the versatility of their catalytic reactions. Peroxidase-mediated reactions can convert the employed immunoreagents into specific products, which can be detected using various methods, including colorimetry, fluorimetry, and chemiluminescence (CL) [7–10]. Among these, CL has emerged as a particularly

promising strategy because of its superior sensitivity, rapid reaction kinetics, and broad dynamic linear range compared to other detection methods. CL-based immunoassays (CLIAs) have thus gathered intense interest and have been used for the quantitative detection of a wide range of analytes, including environmental pollutants, vitamins, proteins, and nucleic acids, as well as CRP [11–17]. However, the effectiveness of CLIAs heavily depends on the luminogenic substances employed, which directly impact the intensity and stability of the CL signal [18]. Luminol, a widely recognized CL reagent, has been conventionally utilized in various bioanalytical applications due to its ability to emit light in the presence of an oxidizing agent, typically hydrogen peroxide (H_2O_2) [19]. Despite its popularity, the efficiency of luminol-based CL reactions was hindered by factors such as signal quenching and insufficient light intensity, especially in complex biological matrices. To address these challenges, the integration of nanomaterials with luminol has been explored as a strategy to enhance the CL signal [20–22].

Nanomaterials offer unique physicochemical properties, such as a high surface-to-volume ratio, quantum confinement effects, and catalytic activities, that can be essentially utilized to improve the performance of CL-based assays [23,24]. Among the various nanomaterials, graphene oxide (GO), a two-dimensional carbon-based nanomaterial, has gained significant attention in the field of biosensing due to its exceptional properties, including its large surface area, excellent conductivity, and ability to interact with a wide range of molecules through π-π stacking, hydrogen bonding, and electrostatic interactions [25–27]. These characteristics make GO an ideal platform for the development of hybrid materials that integrate multiple functional components, leading to synergistic effects that can significantly enhance CL performance [28]. The incorporation of gold nanoparticles (AuNPs) further augments this platform by providing catalytic properties that can amplify the CL signal and by facilitating the interaction between luminol and oxidizing agents such as H_2O_2 [20].

In this study, we explore the potential of a hybrid material, co-functionalized with luminol and AuNPs on a GO surface (GO-AuNPs-L), to serve as an enhanced luminogenic molecule for CLIAs targeting CRP (Scheme 1). This hybrid material is evaluated across two distinct platforms: the well plate-based platform, widely used in clinical laboratories, and the lateral flow immunoassay (LFIA), a point-of-care (POC) diagnostic tool known for its simplicity, portability, and rapid results. GO not only provides a large surface area for the uniform distribution of luminol and AuNPs but also facilitates electron transfer, thereby enhancing the overall CL efficiency. The incorporation of AuNPs is expected to further amplify the signal through catalytic effects and by facilitating the interaction between luminol and the oxidizing agents used in the CL reaction. By leveraging the combined properties of GO, AuNPs, and luminol, the GO-AuNPs-L hybrids were designed to produce a stronger, more stable CL signal, thereby significantly enhancing the sensitivity of CRP detection across both platforms.

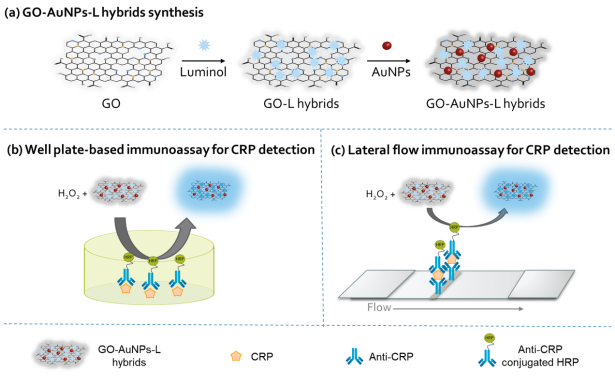

Scheme 1. Schematic illustration of (**a**) the fabrication process of GO-AuNPs-L hybrids and their applications in immunoassays for targeting CRP on a (**b**) well plate-based platform and (**c**) lateral flow immunoassay using GO-AuNPs-L hybrids as luminogenic molecules.

2. Materials and Methods

2.1. Materials

Graphene oxide (GO) (2 mg/mL), chloroauric acid tetrahydrate ($HAuCl_4 \bullet 4H_2O$), luminol, sodium borohydride ($NaBH_4$), cysteamine, HRP, 1-ethyl-3-(3-dimethylaminopropyl) carbodiimide (EDC), N-hydroxysulfosuccinimide (sulfo-NHS), boric acid, phosphoric acid, acetic acid, phosphate-buffered saline (PBS), Tris-HCl buffer, tween 20, glucose, acetylcholine, bovine serum albumin (BSA), and myoglobin (Myo) were purchased from Sigma-Aldrich (St. Louis, MO, USA). H_2O_2 solution was purchased from Samchun chemicals (Seoul, Republic of Korea). CRP antibody (anti-CRP) conjugated HRP was purchased from Abcam (Cambridge, UK). Maxibinding white immunoplate for conducting immunoassay was purchased from SPL science (Pocheon, Gyeonggi, Republic of Korea). Aluminum sealing tape for incubating immunoplate was purchased from Thermofisher Korea (Seoul, Republic of Korea). LFIA nitrocellulose pad, including anti-CRP (2 mg/mL) on T line with or without goat anti-mouse IgG (1 mg/mL) on C line, and CRP were purchased from Boreda Biotech (Seongnam, Republic of Korea). All solutions were prepared with deionized water purified by a Milli-Q Purification System (Millipore, Darmstadt, Germany).

2.2. Synthesis and Characterization of GO-AuNPs-L Hybrids

In this study, AuNPs and GO-AuNPs-L hybrids were synthesized using a slightly modified method based on a previous procedure [20]. Initially, AuNPs were synthesized by adding 400 μL of cysteamine (213 mM) solution into 40 mL of $HAuCl_4$ (1.42 mM) aqueous solution. This mixture was stirred at room temperature (RT) for 20 min, after which 10 μL of a 10 mM $NaBH_4$ solution was added. The resulting mixture was then stirred vigorously in the dark until it turned a wine-red color, indicating the formation of AuNPs. The prepared AuNPs were subsequently stored at 4 °C.

The fabrication of GO-AuNPs-L hybrids was carried out using a physical method to integrate pure GO, pre-synthesized AuNPs, and luminol. Briefly, an aqueous stock solution of GO was sonicated thoroughly to achieve a uniform dispersion, resulting in a final concentration of 0.01 mg/mL. Subsequently, 4 mL of 0.01 M luminol was added to the dispersed GO solution, and the mixture was stirred at RT for 4 h to promote a complete interaction between GO and luminol, forming the GO-L hybrids. Next, 2 mL of previously prepared AuNPs was slowly introduced to the GO-L hybrids under vigorous stirring at RT, and the mixture was then continuously stirred for an additional 12 h to facilitate the formation of the GO-AuNPs-L hybrids. The resulting GO-AuNPs-L hybrids were centrifuged at 10,000 rpm for 10 min to remove any unloaded molecules, and the precipitates were resuspended in distilled water. The stable aqueous solution obtained was stored at 4 °C for subsequent use. As a control to chemically conjugate GO and luminol, GO (0.01 mg/mL) was first washed with MES buffer (0.1 M pH 6.0) and resuspended in the same buffer contained EDC (90 mM) and sulfo-NHS (5 mM). After incubation under shaking conditions for 1 h, the activated GO was centrifuged and washed twice with PBS buffer (0.1 M, pH 7.0) to remove excess reagents. Subsequently, luminol (0.01 M) was added to the GO suspension, and the mixture was shaken at 200 rpm at RT for 1 h, allowing luminol to covalently bind to the activated GO, forming GO-L hybrids. The GO-L hybrids were then thoroughly washed with PBS buffer three times to remove any unreacted luminol and resuspended in the same buffer. The functionalization of AuNPs onto the chemically synthesized GO-L hybrids followed a procedure similar to that described in the physical method.

The morphology of the synthesized GO-AuNPs-L hybrids was analyzed using a transmission electron microscope (TEM, Tecnai, Hillsboro, OR, USA). Fourier transform infrared spectroscopy (FT-IR) was performed using an FT-IR spectrometer (FT/IR-4600, JASCO, Easton, MD, USA) to identify and confirm the chemical functional groups present in the GO-AuNPs-L hybrids.

2.3. CL Measurements

CL intensities of GO-AuNPs-L hybrids, control hybrids, and free luminol were measured in white 96-well plates using a microplate reader (Synergy H1, BioTek, Winooski, VT, USA) serviced by the Center for Bionano Materials Research at Gachon University (Seongnam, Republic of Korea). Typically, 20 μL of HRP (20 ng/mL) and 20 μL of H_2O_2 (10 mM) is added to each well of the well plate containing 140 μL of Britton–Robinson buffer (B-R buffer, pH 9.0). The CL intensities were measured immediately after adding 20 μL of hybrids or 20 μL of free luminol (0.01 M).

2.4. CL Immunoassays for CRP Detection

2.4.1. Well Plate-Based Immunoassay for CRP

The experiments were conducted using a 96-well immunoplate to evaluate the CL response of GO-AuNPs-L hybrids in the detection of CRP. To begin, the wells of the immunoplate were coated with serially diluted CRP, ranging from 20 to 5000 ng/mL, with each well receiving 100 μL of the CRP solution. The plate was then incubated at 37 °C for 2 h under shaking conditions to ensure the binding of CRP to the well surfaces. After incubation, these wells were thoroughly washed with PBST (PBS containing 0.05% tween 20) to remove any unbound CRP and blocked with 3% BSA for 2 h at 37 °C, followed by further washing with TPBS. Subsequently, 100 μL of anti-CRP conjugated HRP was added into each well and continuously incubated at 37 °C for 1 h. Following further washing with PBST, 200 μL of CL solution containing GO-AuNPs-L hybrids, H_2O_2, and Tris-HCl buffer (with the ratio 1:1:1) was introduced to the wells. The CL intensity was recorded immediately using the microplate reader.

To investigate the selectivity toward target CRP, CRP was replaced with the interfering substances such as glucose (Glu), acetylcholine (Ach), BSA, myoglobin (Myo), and SARS-CoV-2 capsid protein (Covid) and further processes were the same as described above.

2.4.2. LFIA for CRP

The commercial LFIA pads specifically designed for CRP detection were utilized. These pads contained a T line coated with anti-CRP (2 mg/mL) with/without a C line coated with goat anti-mouse IgG (1 mg/mL). The pad was then cut into 4 mm wide strips and kept in the desiccator for further use. To assess the performance of LFIA, sample solutions that contained varying concentrations of CRP, along with anti-CRP-conjugated HRP and a buffer solution (0.04 M PBS containing 0.6% tween 20), were prepared. The LFIA test strips were then immersed in these sample solutions for 10 min at RT. After the incubation period, a CL solution containing GO-AuNPs-L hybrids, H_2O_2, and Tris-HCl buffer (in a 1:1:1 ratio) was then applied to the test strips. Immediately following the CL reaction, the reacted strips were imaged using a CL imaging system (UVITEC, Cambridge, UK). The captured images were then converted to gray scale, which was subjected to quantitative image processing with ImageJ software (NIH).

To evaluate the selectivity of the LFIA platform toward the target CRP, negative control experiments were conducted in which the sample solutions included potential interfering substances such as Glu, Ach, BSA, Myo, and the Covid. These experiments were processed in the same manner as described above.

3. Results and Discussion

3.1. Construction of GO-AuNPs-L Hybrids

The synthesis of GO-AuNPs-L hybrids was achieved through physical adsorption, starting with the preparation of AuNPs by the facile incubation of cysteamine with gold precursor at RT, and $NaBH_4$ was used as a reducing agent. Afterwards, GO-AuNPs-L hybrids were developed by sequentially mixing luminol and AuNPs into GO aqueous solution. The positive charge of the AuNPs promotes their adsorption onto the negatively charged GO sheets, while luminol binds to GO primarily through π-π stacking interactions. Control groups, including GO-AuNPs, GO-L, and AuNPs-L hybrids, were also prepared

using a similar physical adsorption procedure, with variations in the absence of luminol, AuNPs, or GO, respectively.

Due to the addition of GO, the synthesized GO-AuNPs-L hybrids had a black color, while the AuNPs showed a reddish color (Figure 1a). The hybrids were characterized using TEM and FT-IR. TEM analysis confirmed the characteristic spherical morphology of the AuNPs, which were uniformly distributed on the surface of the GO sheets, thereby validating the successful functionalization of GO with AuNPs and luminol (Figure 1c–e). From the FT-IR spectra, the typical peaks of GO were observed in GO-AuNPs-L and GO-L hybrids, such as the peaks at 1775 cm^{-1}, 1454 cm^{-1}, and 1069 cm^{-1}, corresponding to the C=O stretching vibrations of the–COOH groups, C–OH groups, and C–O–C in the epoxide groups, respectively [29]. Moreover, a markedly broad peak at 3417 cm^{-1} was observed, indicating primary amine (N–H) stretching vibrations, which are characteristic of luminol. Additionally, peaks at 2853 cm^{-1} and 2923 cm^{-1} were attributed to the valence vibrations (υC–H) of the benzene ring in luminol (Figure 1b) [30]. The presence of these characteristic peaks in the FT-IR spectra of the GO-AuNPs-L hybrids, along with the control groups GO-L and AuNPs-L hybrids, confirms the incorporation of luminol into the hybrids. These results collectively demonstrated the successful synthesis of GO-AuNPs-L hybrids through physical adsorption with the typical morphology and chemical characteristics of their constituent components, such as GO, AuNPs, and luminol.

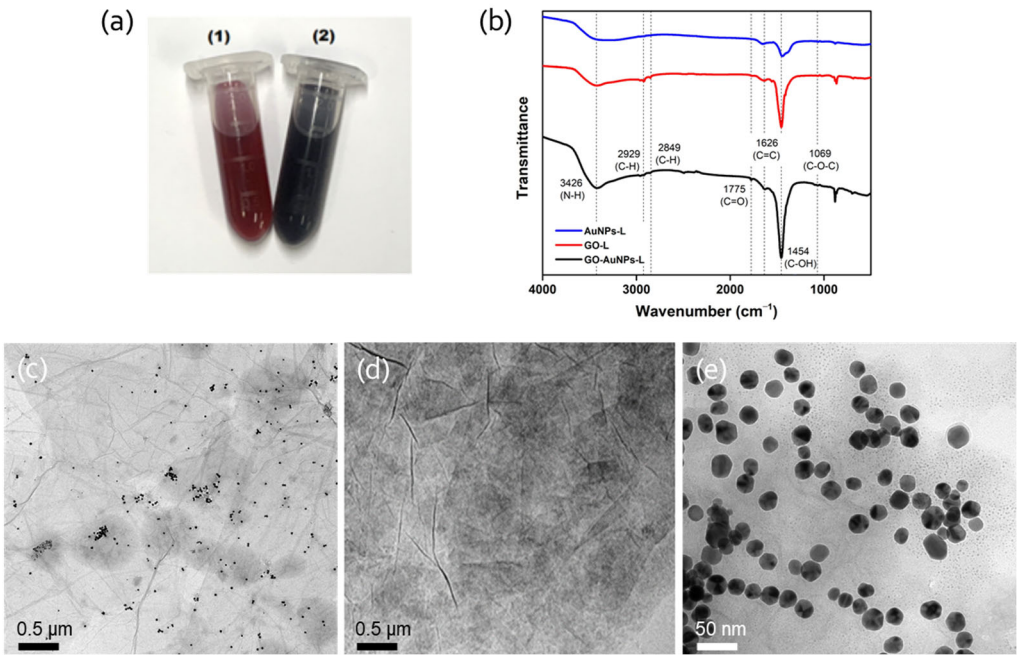

Figure 1. (**a**) Real image of (1) AuNPs and (2) GO-AuNPs-L hybrids. (**b**) FT-IR spectra and TEM images of (**c**) GO-AuNPs-L hybrids, (**d**) GO-L hybrids, and (**e**) AuNPs-L hybrids.

3.2. Enhanced CL of GO-AuNPs-L Hybrids

The CL properties of the GO-AuNPs-L hybrids were evaluated to determine their effectiveness as luminogenic molecules in peroxidase-catalyzed reactions. In the reactions, HRP reacts with H_2O_2 to initiate the formation of multiple radical species, which subsequently oxidize luminol to produce a strong CL signal. To optimize the CL performance, the effects of pH on the system were examined. The results revealed that the highest CL activity was achieved at pH 9.0, which was selected as the optimal pH for subsequent experiments (Figure S1). It is presumed that luminol in GO-AuNPs-L hybrids would become dianionic under basic pH conditions, which can subsequently be oxidized to produce CL signals [19]. In addition, the CL behaviors of GO-AuNPs-L were compared with several control groups, including GO-L, AuNPs-L, a mixture of GO-AuNPs and free luminol, and

free luminol. Additionally, GO-AuNPs-L hybrids that were covalently bonded through the EDC/sulfo-NHS method were also included as a comparison group. As shown in Figure 2, GO-AuNPs-L hybrids exhibited the highest and most sustained CL intensity. Specifically, the CL intensity of GO-AuNPs-L hybrids was over five times greater than that of free luminol. Moreover, the CL signal generated by the GO-AuNPs-L hybrids was not only stronger but also more persistent, maintaining its intensity for up to 30 min, whereas the signal from free luminol diminished over time (Figure S2). The enhanced and prolonged CL signal observed with the GO-AuNPs-L hybrids can be attributed to the synergistic effects of AuNPs and GO. AuNPs likely facilitate efficient electron transfer during the luminol oxidation process, enhancing the CL signal. Meanwhile, GO serves as an effective carrier offering a unique planar π–network reaction interface and accelerating radical generation and electron transfer during the chemical reaction, leading to a high yield of radical formation and, consequently, a stronger and more persistent CL signal [20]. The incorporation of AuNPs and luminol onto the GO surface markedly enhances both the intensity and duration of the CL signal. This improvement is particularly advantageous for POC applications, where a robust and reliable CL signal is essential for accurate and sensitive detection.

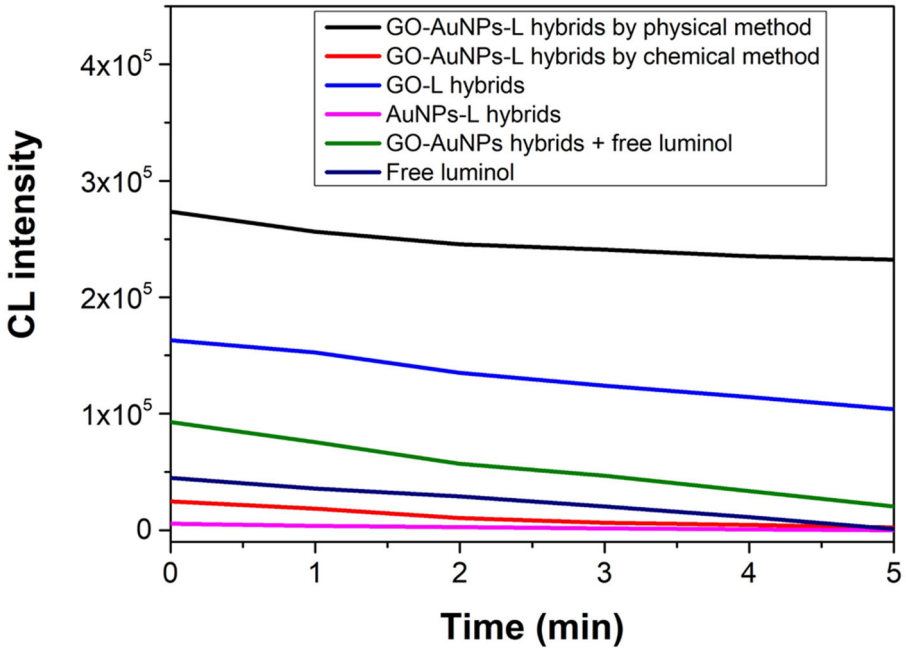

Figure 2. CL intensity of GO-AuNPs-L hybrids and control materials (GO-AuNPs-L hybrids synthesized by chemical method, GO-L hybrids, Au-L hybrids, mixture of GO-AuNPs hybrids + free luminol, and free luminol) in B-R buffer at pH 9.

3.3. CL Immunoassay for CRP Using GO-AuNPs-L Hybrids as Luminogenic Reagents

Thanks to the superior CL properties of GO-AuNPs-L hybrids, the hybrids were employed as an alternative luminogenic substance in constructing a GO-AuNPs-L hybrid and H_2O_2-HRP system-based immunoassay for the detection of CRP. The immunoassay was implemented on two distinct platforms: the well plate-based format (off-device assay) and the LFIA platform.

3.3.1. Well Plate-Based Immunoassay for CRP

For the well plate-based assay, a direct CLIA for the determination of CRP was designed using anti-CRP conjugated HRP as a capture antibody and GO-AuNPs-L hybrids as CL signal generators. The optimization of experimental conditions, including the concentration of anti-CRP conjugated HRP and H_2O_2, was essential for maximizing assay performance. The results indicated that the highest CL intensity was achieved with

10 μg/mL of anti-CRP conjugated HRP and 100 mM H_2O_2 (Figure S3), which were determined to be the optimal concentrations for the well plate-based immunoassay. Under the optimized conditions, the selectivity toward target CRP by GO-AuNPs-L hybrids-based immunoassay was evaluated. A high concentration of the potential interferences in human serum, including Glu, Ach, BSA, Myo, and Covid, were tested to fully demonstrate the specificity of the system toward the target CRP. Notably, a strong CL intensity was obtained exclusively in the presence of CRP, while no detectable CL signal from other interferences, even at concentrations 10-fold higher than CRP (Figure 3a). These results demonstrate the high selectivity of the system for CRP detection. As the concentrations of CRP increased, the corresponding CL intensities increased gradually (Figure 3b). Based on the linear calibration plots, the limit of detection (LOD) for CRP was determined to be as low as 5.1 ng/mL, with the linear ranges extending up to 1000 ng/mL.

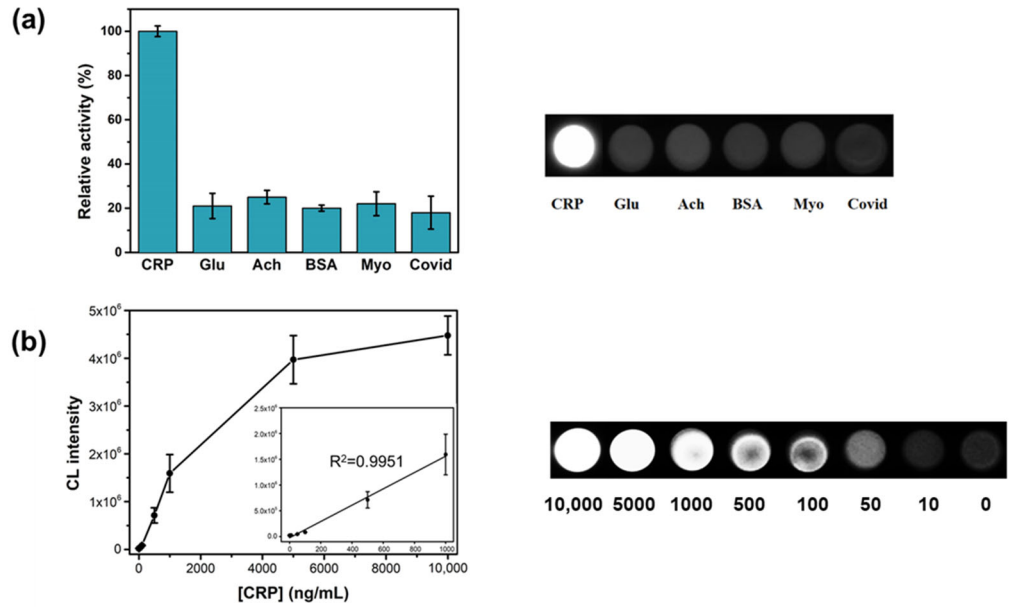

Figure 3. (**a**) Selectivity of well plate-based immunoassay for detecting CRP. CRP was used at 5 μg/mL, whereas all control samples were used at 50 μg/mL. (**b**) Sensitivity of well plate-based immunoassay for detecting CRP. Dose–response curves and the corresponding linear calibration plots are presented. Photographs show images of the well plates.

3.3.2. LFIA for CRP

The LFIA strips were developed to enable the CL determination of CRP. In the presence of CRP in a sample solution, the anti-CRP conjugated HRP was captured on the T lines through the antigen–antibody interaction. Upon addition of the CL solution containing H_2O_2 and GO-AuNPs-L hybrids to the test line, a detectable CL signal was produced. The LFIA strips were imaged using a UVITEC machine, and quantitative analysis was performed using ImageJ software. For developing an efficient LFIA, the concentrations of anti-CRP conjugated HRP and H_2O_2 were optimized. The highest CL intensity ratio was achieved with 1 μg/mL of anti-CRP conjugated HRP and 10 mM H_2O_2 (Figure S4). Under these conditions, the GO-AuNPs-L hybrid and H_2O_2-HRP system-based LFIA effectively detected target CRP, with a strong luminescent signal corresponding to increasing CRP concentrations (Figure 4a). In contrast, negative control samples exhibited negligible intensities even at 10-fold higher concentrations than the target CRP, aligning with the results from the well plate assay. As the concentration of CRP increased, the intensity gradually increased (Figure 4b), yielding an effective working dynamic range of up to ~100 ng/mL. From the linear calibration analysis, the LOD value was calculated to be 10 ng/mL. Although the LOD and linear range values of GO-AuNPs-L hybrid and H_2O_2-HRP system-based immunoassay are not the best when compared with the recent CRP

detection sensors, the developed system fulfills the diagnostic requirements to detect CRP in human serum with higher signal stability (Table S1) [4,31–36]. The reproducibility and accuracy of the GO-AuNPs-L hybrid and H_2O_2-HRP system-based LFA were assessed using the GO-AuNPs-L hybrids synthesized from three different batches. The results showed that the intra-coefficient of variation (intra-CV) and inter-CV among different batches were 4.11–7.63% and 5.51%, respectively, demonstrating the high reproducibility of the current system (Table S2). Moreover, high recovery (100.22–100.97%) was achieved, showing the sufficient accuracy of the developed LFIA for CRP. These results confirmed that the proposed GO-AuNPs-L hybrids-based immunoassay is a promising tool for both well plate-based and LFIA platforms, providing a robust and sensitive method for CRP detection in POC settings. The enhanced CL performance of the GO-AuNPs-L hybrids underscores their potential for effective and reliable biomarker detection in various diagnostic applications.

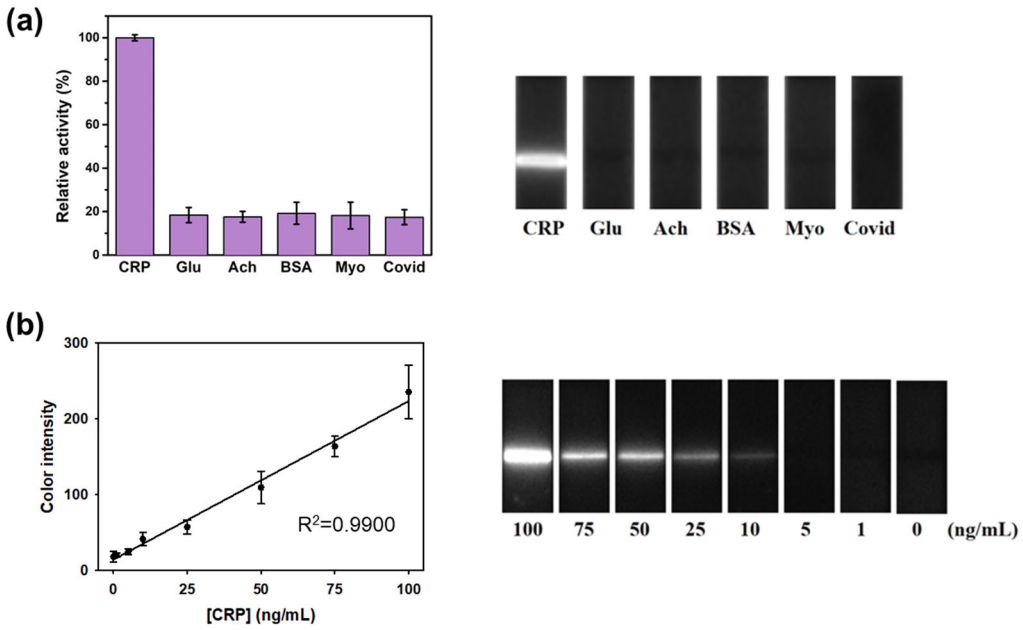

Figure 4. (**a**) Selectivity of LFIA for detecting CRP. CRP was used at 100 ng/mL, whereas all control samples were used at 1000 ng/mL. (**b**) Sensitivity of LFIA for detecting CRP. Photographs show images of the test strips.

4. Conclusions

In conclusion, we demonstrated that the GO modified with luminol and AuNPs, forming GO-AuNPs-L hybrids, significantly enhances CL activity compared to free luminol. The GO-AuNPs-L hybrids exhibited not only a markedly stronger CL signal but also a prolonged and stable luminescence, marking a notable improvement over traditional luminol-based systems. This improvement is attributed to the synergistic effects of GO, AuNPs, and luminol, which collectively enhance the efficiency of the CL reaction. The successful application of GO-AuNPs-L hybrids in CLIAs for the detection of CRP has been validated on both well plate-based and LFIA platforms. The superior sensitivity and reliability provided by these hybrids underscore their versatility and effectiveness in various diagnostic settings, highlighting their potential for broader use in diverse diagnostic applications.

Supplementary Materials: The following supporting information can be downloaded at https://www.mdpi.com/article/10.3390/chemosensors12090193/s1, Figure S1: Effects of buffer pH on the CL intensity of GO-AuNPs-L hybrids; Figure S2: CL intensities of GO-AuNPs-L hybrids and free luminol over 30 min at RT; Figure S3: Optimization of (a) anti-CRP-HRP and (b) H_2O_2 concentration to detect CRP using well plate-based immunoassay; Figure S4: Optimization of (a) anti-CRP-HRP and (b) H_2O_2 concentration to detect CRP using LFIA; Table S1: Comparison of analytical performances of

GO-AuNPs-L hybrids-H_2O_2-HRP system-based LFIA with recently reported LFIA-based CRP detection; and Table S2: Reproducibility and accuracy of GO-AuNPs-L hybrids-H_2O_2-HRP system-based LFIA for CRP detection. References [4,31–36] are cited in the Supplementary Materials.

Author Contributions: Conceptualization, K.M.K. and M.I.K.; investigation, K.M.K., P.T.N., J.K., S.H.S. and J.W.P.; validation, J.K. and S.H.S.; writing—original draft preparation, K.M.K. and P.T.N.; writing—review and editing, J.W.P. and M.I.K.; supervision, M.I.K. All authors have read and agreed to the published version of the manuscript.

Funding: This work was supported by the Starting Growth Technological R&D Program (RS-2023-00256609) funded by the Ministry of SMEs and Startups (MSS, Republic of Korea). This research was also supported by a National Research Foundation of Korea (NRF) grant funded by the Korean government (Ministry of Science and ICT [NRF-2023R1A2C2007833]) and the Gachon University research fund of 2021 (GCU-202110350001).

Institutional Review Board Statement: Not applicable.

Informed Consent Statement: Not applicable.

Data Availability Statement: Data are contained within the article and Supplementary Materials.

Conflicts of Interest: Author Jin Woo Park was employed by BioActs BM&S Co., Ltd. The remaining authors declare that the research was conducted in the absence of any commercial or financial relationships that could be construed as potential conflicts of interest.

References

1. Ridker, P.M.; Glynn, R.J.; Hennekens, C.H. C-reactive protein adds to the predictive value of total and HDL cholesterol in determining risk of first myocardial infarction. *Circulation* **1998**, *97*, 2007–2011. [CrossRef] [PubMed]
2. Ridker, P.M. High-sensitivity C-reactive protein, inflammation, and cardiovascular risk: From concept to clinical practice to clinical benefit. *Am. Heart J.* **2004**, *148*, S19–S26. [CrossRef] [PubMed]
3. Sweeney, T.; Quispe, R.; Das, T.; Juraschek, S.P.; Martin, S.S.; Michos, E.D. The Use of Blood Biomarkers in Precision Medicine for the Primary Prevention of Atherosclerotic Cardiovascular Disease: A Review. *Expert. Rev. Precis. Med. Drug Dev.* **2021**, *6*, 247–258. [CrossRef] [PubMed]
4. Kong, D.Y.; Heo, N.S.; Kang, J.W.; Lee, J.B.; Kim, H.J.; Kim, M.I. Nanoceria-based lateral flow immunoassay for hydrogen peroxide-free colorimetric biosensing for C-reactive protein. *Anal. Bioanal. Chem.* **2022**, *414*, 3257–3265. [CrossRef] [PubMed]
5. Pohanka, M. Diagnoses based on C-reactive protein point-of-care tests. *Biosensors* **2022**, *12*, 344. [CrossRef]
6. Siddiqui, M.F.; Khan, Z.A.; Park, S. Detection of C-reactive protein using histag-HRP functionalized nanoconjugate with signal amplified immunoassay. *Nanomaterials* **2020**, *10*, 1240. [CrossRef]
7. Zhang, Z.; Lai, J.; Wu, K.; Huang, X.; Guo, S.; Zhang, L.; Liu, J. Peroxidase-catalyzed chemiluminescence system and its application in immunoassay. *Talanta* **2018**, *180*, 260–270. [CrossRef]
8. Zhou, Y.; Huang, X.; Xiong, S.; Li, X.; Zhan, S.; Zeng, L.; Xiong, Y. Dual-mode fluorescent and colorimetric immunoassay for the ultrasensitive detection of alpha-fetoprotein in serum samples. *Anal. Chim. Acta* **2018**, *1038*, 112–119. [CrossRef]
9. Darwish, I.A.; Alzoman, N.Z.; Khalil, N.N. A Novel Highly Sensitive Chemiluminescence Enzyme Immunoassay with Signal Enhancement Using Horseradish Peroxidase-Luminol-Hydrogen Peroxide Reaction for the Quantitation of Monoclonal Antibodies Used for Cancer Immunotherapy. *Chemosensors* **2023**, *11*, 245. [CrossRef]
10. Liu, Z.J.; Wang, X.Y.; Ren, X.X.; Li, W.B.; Sun, J.F.; Wang, X.W.; Huang, Y.Q.; Guo, Y.G.; Zeng, H.W. Novel Fluorescence Immunoassay for the Detection of Zearalenone Using Hrp-Mediated Fluorescence Quenching of Gold-Silver Bimetallic Nanoclusters. *Food Chem.* **2021**, *355*, 129633. [CrossRef]
11. Zhang, C.; Su, Y.; Liang, Y.; Lai, W.; Jiang, J.; Wu, H.; Mao, X.; Zheng, L.; Zhang, R. Chemiluminescence and Its Biomedical Applications. In *Nanophotonics in Biomedical Engineering*; Zhao, X., Lu, M., Eds.; Springer: Singapore, 2021; pp. 143–195.
12. Li, F.; You, M.; Li, S.; Hu, J.; Liu, C.; Gong, Y.; Yang, H.; Xu, F. Paper based point-of-care immunoassays: Recent advances and emerging trends. *Biotechnol. Adv.* **2020**, *39*, 107442. [CrossRef]
13. Zhao, L.; Xu, J.; Xiong, L.; Wang, S.; Yu, C.; Lv, J.; Lin, J.-M. Recent development of chemiluminescence for bioanalysis. *TrAC Trends Anal. Chem.* **2023**, *166*, 117213. [CrossRef]
14. Islam, M.S.; Kang, S.H. Chemiluminescence detection of label-free C-reactive protein based on catalytic activity of gold nanoparticles. *Talanta* **2011**, *84*, 752–758. [CrossRef] [PubMed]
15. Luo, Y.; Zhang, B.; Chen, M.; Jiang, T.; Zhou, D.; Huang, J.; Fu, W. Sensitive and rapid quantification of C-reactive protein using quantum dot-labeled microplate immunoassay. *J. Transl. Med.* **2012**, *10*, 24. [CrossRef] [PubMed]
16. Ghavamipour, F.; Rahmani, H.; Shanehsaz, M.; Khajeh, K.; Mirshahi, M.; Sajedi, R.H. Enhanced Sensitivity of VEGF Detection Using Catalase-Mediated Chemiluminescence Immunoassay Based on CdTe QD/H_2O_2 System. *J. Nanobiotechnol.* **2020**, *18*, 93. [CrossRef]

17. Al Yahyai, I.; Al-Lawati, H.A. A review of recent developments based on chemiluminescence detection systems for pesticides analysis. *Luminescence* **2021**, *36*, 266–277. [CrossRef] [PubMed]
18. Tao, X.; Wang, W.; Wang, Z.; Cao, X.; Zhu, J.; Niu, L.; Wu, X.; Jiang, H.; Shen, J. Development of a highly sensitive chemiluminescence enzyme immunoassay using enhanced luminol as substrate. *Luminescence* **2014**, *29*, 301–306. [CrossRef] [PubMed]
19. Khan, P.; Idrees, D.; Moxley, M.A.; Corbett, J.A.; Ahmad, F.; von Figura, G.; Sly, W.S.; Waheed, A.; Hassan, M.I. Luminol-based chemiluminescent signals: Clinical and non-clinical application and future uses. *Appl. Biochem. Biotechnol.* **2014**, *173*, 333–355. [CrossRef]
20. Lin, K.L.; Yang, T.; Zhang, F.F.; Lei, G.; Zou, H.Y.; Li, Y.F.; Huang, C.Z. Luminol and gold nanoparticle-co-precipitated reduced graphene oxide hybrids with long-persistent chemiluminescence for cholesterol detection. *J. Mater. Chem. B* **2017**, *5*, 7335–7341. [CrossRef]
21. Chen, H.; Wang, Q.; Shen, Q.; Liu, X.; Li, W.; Nie, Z.; Yao, S. Nitrogen doped graphene quantum dots based long-persistent chemiluminescence system for ascorbic acid imaging. *Biosens. Bioelectron.* **2017**, *91*, 878–884. [CrossRef]
22. Gao, J.-W.; Chen, M.-M.; Wen, W.; Zhang, X.; Wang, S.; Huang, W.-H. Au-Luminol-decorated porous carbon nanospheres for the electrochemiluminescence biosensing of MUC1. *Nanoscale* **2019**, *11*, 16860–16867. [CrossRef] [PubMed]
23. Zhu, H.; Huang, X.; Deng, Y.; Chen, H.; Fan, M.; Gong, Z. Applications of nanomaterial-based chemiluminescence sensors in environmental analysis. *Trac-Trend. Anal. Chem.* **2022**, *158*, 116879. [CrossRef]
24. Teng, X.; Qi, L.; Liu, T.; Li, L.; Lu, C. Nanomaterial-based chemiluminescence systems for tracing of reactive oxygen species in biosensors. *Trac-Trend. Anal. Chem.* **2023**, *162*, 117020. [CrossRef]
25. Jiang, X.; Ruan, G.; Huang, Y.; Chen, Z.; Yuan, H.; Du, F. Assembly and application advancement of organic-functionalized graphene-based materials: A review. *J. Sep. Sci.* **2020**, *43*, 1544–1557. [CrossRef] [PubMed]
26. Shahriari, S.; Sastry, M.; Panjikar, S.; Singh Raman, R. Graphene and Graphene Oxide as a Support for Biomolecules in the Development of Biosensors. *Nanotechnol. Sci. Appl.* **2021**, *14*, 197–220. [CrossRef]
27. Gosai, A.; Khondakar, K.R.; Ma, X.; Ali, M.A. Application of functionalized graphene oxide based biosensors for health monitoring: Simple graphene derivatives to 3D printed platforms. *Biosensors* **2021**, *11*, 384. [CrossRef]
28. Yang, L.; Zhang, R.; Liu, B.; Wang, J.; Wang, S.; Han, M.Y.; Zhang, Z. π-Conjugated carbon radicals at graphene oxide to initiate ultrastrong chemiluminescence. *Angew. Chem. Int. Ed.* **2014**, *53*, 10109–10113. [CrossRef]
29. Shams, N.; Lim, H.N.; Hajian, R.; Yusof, N.A.; Abdullah, J.; Sulaiman, Y.; Ibrahim, I.; Huang, N.M. Electrochemical sensor based on gold nanoparticles/ethylenediamine-reduced graphene oxide for trace determination of fenitrothion in water. *RSC Adv.* **2016**, *6*, 89430–89439. [CrossRef]
30. Lou, F.; Wang, A.; Jin, J.; Li, Q.; Zhang, S. One-pot synthesis of popcorn-like Au@Polyluminol nanoflowers for sensitive solid-state electrochemiluminescent sensor. *Electrochim. Acta* **2018**, *278*, 255–262. [CrossRef]
31. Guo, J.; Chen, S.; Tian, S.; Liu, K.; Ma, X.; Guo, J. A sensitive and quantitative prognosis of C-reactive protein at picogram level using mesoporous silica encapsulated core-shell up-conversion nanoparticle based lateral flow strip assay. *Talanta* **2021**, *230*, 122335. [CrossRef]
32. Jin, B.; Du, Z.; Zhang, C.; Yu, Z.; Wang, X.; Hu, J.; Li, Z. Eu-chelate polystyrene microsphere-based lateral flow immunoassay platform for hs-CRP detection. *Biosensors* **2022**, *12*, 977. [CrossRef] [PubMed]
33. Wu, R.; Zhou, S.; Chen, T.; Li, J.; Shen, H.; Chai, Y.; Li, L.S. Quantitative and rapid detection of C-reactive protein using quantum dot-based lateral flow test strip. *Anal. Chim. Acta* **2018**, *1008*, 1–7. [CrossRef] [PubMed]
34. Liu, X.; Ren, X.; Chen, L.; Zou, J.; Li, T.; Tan, L.; Fu, C.; Wu, Q.; Li, C.; Wang, J.; et al. Fluorescent hollow ZrO2@CdTe nanoparticles-based lateral flow assay for simultaneous detection of C-reactive protein and troponin T. *Microchim. Acta* **2021**, *188*, 209. [CrossRef] [PubMed]
35. Kokorina, A.A.; Rashchevskaya, R.O.; Goryacheva, I.Y. Nets of biotin-derived gold nanoparticles as a label for the C-reactive protein immunoassay. *Anal. Bioanal. Chem.* **2021**, *413*, 6867–6875. [CrossRef]
36. Panferov, V.G.; Byzova, N.A.; Zherdev, A.V.; Dzantiev, B.B. Peroxidase-mimicking nanozyme with surface-dispersed Pt atoms for the colorimetric lateral flow immunoassay of C-reactive protein. *Microchim. Acta* **2021**, *188*, 309. [CrossRef]